Hypoxic and Reoxygenated Microenvironment: Stemness and Differentiation State in Glioblastoma

Mariana Maier Gaelzer, Mariana Silva dos Santos, Bárbara Paranhos Coelho, Alice Hoffman de Quadros, Fabrício Simão, et al.

Molecular Neurobiology

ISSN 0893-7648

Mol Neurobiol
DOI 10.1007/s12035-016-0126-6

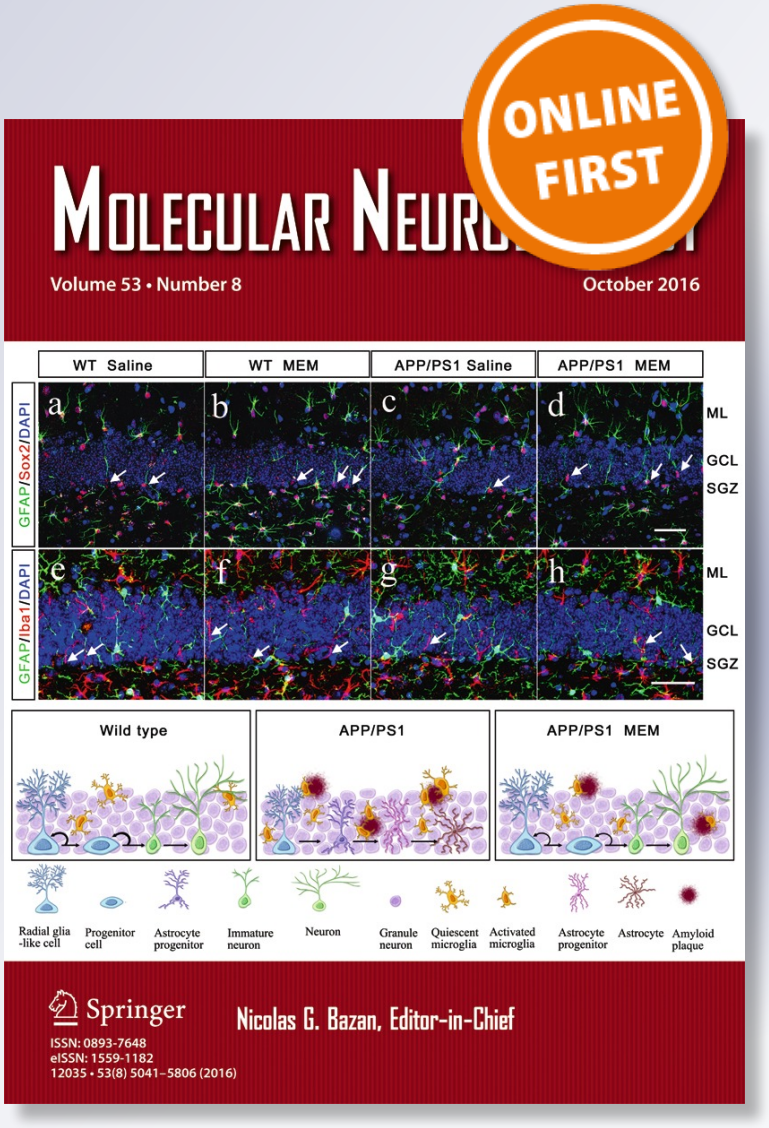

Springer

Mol Neurobiol
DOI 10.1007/s12035-016-0126-6

Hypoxic and Reoxygenated Microenvironment: Stemness and Differentiation State in Glioblastoma

Mariana Maier Gaelzer[1,2] · Mariana Silva dos Santos[1] · Bárbara Paranhos Coelho[1] · Alice Hoffman de Quadros[1] · Fabrício Simão[3] · Vanina Usach[4] · Fátima Costa Rodrigues Guma[1] · Patrícia Setton-Avruj[4] · Guido Lenz[5] · Christianne G. Salbego[1]

Received: 3 August 2016 / Accepted: 12 September 2016

Abstract Glioblastoma (GBM) is the most common and aggressive primary malignant brain tumor in adults. Hypoxia is a distinct feature in GBM and plays a significant role in tumor progression, resistance to treatment, and poor outcome. However, there is lack of studies relating type of cell death, status of Akt phosphorylation on Ser473, mitochondrial membrane potential, and morphological changes of tumor cells after hypoxia and reoxygenation. The rat glioma C6 cell line was exposed to oxygen deprivation (OD) in 5 % fetal bovine serum (FBS) or serum-free media followed by reoxygenation (RO). OD induced apoptosis on both 5 % FBS and serum-free groups. Overall, cells on serum-free media showed more profound morphological changes than cells on 5 % FBS. Moreover, our results suggest that OD combined with absence of serum provided a favorable environment for glioblastoma dedifferentiation to cancer stem cells, since nestin, and CD133 levels increased. Reoxygenation is present in hypoxic tumors through microvessel formation and cell migration to oxygenated areas. However, few studies approach these phenomena when analyzing hypoxia. We show that RO caused morphological alterations characteristic of cells undergoing a differentiation process due to increased GFAP. In the present study, we characterized an in vitro hypoxic microenvironment associated with GBM tumors, therefore contributing with new insights for the development of therapeutics for resistant glioblastoma.

Keywords Cancer · Glioma · Hypoxia · Reoxygenation · C6 · Cancer stem cell

Introduction

Glioblastoma (GBM) is the most common and most lethal form of primary brain tumor. Despite different combinations of treatments, such as radiotherapy and chemotherapy, the average survival for GBM patients is 15 months [1, 2]. These are morphologic, genetic, and phenotypically heterogeneous tumors [3].

GBMs display an elevated proliferation rate with extensive areas of necrosis and hypoxia as a result of this rapid tumor cell growth. Low O_2 levels favor tumor progression through activation of vascular endothelial growth factor (VEGF). In tumor cells, VEGF induces cell proliferation [4] and stimulates cell invasion [5] and is also responsible for maintenance of tumor cells in an undifferentiated phenotype [6].

The tumor microenvironment contains a minor fraction of cancer stem cells (CSCs). CSCs are characterized by self-renewal and maintenance of tumor mass. When transplanted, they are responsible for new tumor growth [7, 8], increased

Mariana Maier Gaelzer and Mariana Silva dos Santos contributed equally to this work.

Electronic supplementary material The online version of this article (doi:10.1007/s12035-016-0126-6) contains supplementary material, which is available to authorized users.

✉ Mariana Maier Gaelzer
marianamaierg@gmail.com

[1] Biochemistry Department, Federal University of Rio Grande do Sul, Porto Alegre, RS, Brazil

[2] Biochemistry Department, Institute of Health Sciences, 2600 Ramiro Barcelos Street, Porto Alegre, RS 90035-003, Brazil

[3] Harvard Medical School Joslin Diabetes Center, Boston, MA, USA

[4] Biological Chemistry Department, University of Buenos Aires, Ciudad Autónoma de Buenos Aires, Argentina

[5] Biophysics Department, Federal University of Rio Grande do Sul, Porto Alegre, RS, Brazil

Published online: 06 October 2016

chemotherapy resistance, and initiation of tumor invasion by stimulating migration of differentiated cancer cells [8, 9].

The C6 cell line is widely used in the study of gliomas. C6 cells contain a pool of cancer stem cells expressing CD133 and nestin [10], which are the established markers for brain CSCs and can be used for isolating them. Moreover, some studies suggest the use of cell size, granularity, and mitochondrial membrane potential for characterization and isolation of CSCs and stem cells in general [11].

The hypoxic environment drives the selection of more aggressive tumor cells through cellular adaptations [12]. Developing an in vitro model of the hypoxic microenvironment allows for a more in-depth study of those adaptations, contributing to the enhancement of therapies against these aggressive tumor cells. In order to mimic a tumor hypoxic niche and to analyze the adaptations of glioma C6 cells to these conditions, we exposed cells to oxygen deprivation (OD) on serum-free medium or with 5 % fetal bovine serum (FBS). We analyzed cell death; morphological changes; and Akt, VEGF, nestin, CD133, and glial fibrillary acidic protein (GFAP) levels during OD. Additionally, we observed morphological changes indicating phenotypic alterations in the cells during reoxygenation (RO) following OD. Our results provide insight into the cellular alterations caused by a hypoxic microenvironment on GBM tumor cells.

Materials and Methods

Chemicals and Materials

Cell culture media and FBS were obtained from Gibco-Invitrogen (Grand Island, NY, USA). Propidium iodide (PI) was obtained from Sigma Chemical Co (St. Louis, MO, USA). All other reagents were purchased from Sigma Chemical Co or Merck (Darmstadt, Germany). All other chemicals and solvents used were of analytical or pharmaceutical grade.

Cell Culture

The C6 rat glioma cell line was obtained from the American Type Culture Collection (Rockville, MD, USA). Cells were grown and maintained in Dulbecco's modified Eagle's Medium (DMEM; Gibco-Invitrogen) supplemented with 5 % (*v*/*v*) FBS (Gibco-Invitrogen) containing 2.5 mg/mL Fungizone and 100 U/L gentamicin (Shering do Brasil, São Paulo, SP, Brazil). Cells were incubated at 37 °C in a minimum relative humidity of 5 % CO_2 atmosphere. Experiments throughout this study were conducted either in serum-free DMEM or in serum-supplemented DMEM.

Oxygen Deprivation

OD was achieved according to the method described by Strasser and Fischer [13] with some modifications [14]. C6 glioma cells were seeded at 4.5×10^3 cells/well in DMEM/5 % FBS in six-well plates and grown for 72 h. Following the 72 h growth, the group that received serum during OD had its medium replaced by conventional 5 % FBS media previously bubbled with N_2 for 30 min. The group that did not receive serum had its medium replaced with serum-free DMEM, also previously bubbled with N_2 for 30 min. Plates were immediately transferred to an anaerobic chamber at 37 °C in a N_2-enriched atmosphere for 15 min, 1 h, or 3 h. Controls were maintained in an incubator with 5 % CO_2 atmosphere at 37 °C.

Flow Cytometry Analysis

Flow cytometry was used to evaluate size and granularity of cells, cell death, proteins levels, and mitochondrial mass and membrane potential. After OD, culture medium and cells were harvested with trypsin. Cells were then evaluated for size and granularity using the forward-scatter (FSC) and side-scatter (SSC) light parameters and stained with dyes or incubated with the proper antibodies for flow cytometry analysis using a FACSCalibur flow cytometer (Becton Dickinson, Franklin Lakes, NJ, USA). Analysis was performed using the FCS Express 5 software (De Novo Software, Los Angeles, CA, USA).

Classification of Cell Death

Apoptotic and necrotic cell deaths were analyzed by flow cytometry by double staining with fluorescein isothiocyanate (FITC)-conjugated annexin V and PI for 20 min. Staining was performed according to the manufacturer's instructions (BD Pharmingen, San Diego, CA, USA). Flow cytometry analysis was performed as described in "Flow Cytometry Analysis" section.

Classification of Cell Size and Granularity

As the population of cells appeared to be morphologically heterogeneous, parameters of cell size and granularity were measured by flow cytometry and plotted against markers of cell death. Cells were divided into three subpopulations based on size: small (S), medium (M), and large (L). To assess the distribution of granularity between viable and dead cells, cells were divided into two subpopulations based on flow cytometry

analysis according to their granularity: regular (G1) and granular (G2).

Immunodetection

To investigate cellular adaptations to hypoxia, key proteins were studied. After OD and RO periods, cells were fixed with phosphate-buffered saline (PBS) and 4 % paraformaldehyde for 20 min, then cells were permeabilized with PBS and 0.01 % Triton X-100 and/or incubated with the primary antibodies anti-VEGF (1:100; Santa Cruz Biotech, Dallas, TX, USA), anti-Akt (1:50; Cell Signaling Technology™, Beverly, MA, USA), anti-p-Akt_{Ser473} (1:50; Cell Signaling Technology™), anti-nestin (1:50; Cell Signaling Technology™), anti-GFAP (1:50; Cell Signaling Technology™), and anti-CD133 (1:50; Cell Signaling Technology™) for 30 min. The secondary antibody, Alexa Fluor 488 anti-mouse or Alexa Fluor 555 anti-mouse (1:100; Gibco-Invitrogen), was added, and after a 60 min incubation, cells were analyzed by flow cytometry.

MitoTracker Staining

Mitochondrial mass and membrane potential were evaluated using MitoTracker® Green and MitoTracker® Red (Invitrogen®, Molecular Probes, Eugene, OR, USA), respectively. Cells were incubated in a PBS/MitoTracker Green/Red solution (100 nM) at 37 °C, in the dark, for 45 min.

Microscopy

To identify cell death, 5 μM PI and 2.5 μM 4′,6-diamidino-2-phenylindole (DAPI) was added to C6 glioma cells after induction of OD. PI fluorescence was excited at 515–560 nm using an inverted microscope (Nikon Eclipse TE300; Nikon, Tokyo, Japan) fitted with a standard rhodamine filter. For nucleous stain 2.5 μM of DAPI was added. DAPI was excited by the violet 405 nm laser line, and images were captured using a digital camera connected to the microscope. Sulforhodamine B (SRB) assay was used for staining cell proteins. Cells were fixed with PBS/FORMOL 4 % for 15 min and stained with SRB. Unbound stain was washed, and cells were analyzed on an Olympus FV1000 laser scanning confocal microscope. All images were processed with ImageJ software (NIH, Bethesda, MD, USA).

Reoxygenation Assay

OD was performed in serum-free medium for 15 min, 1 h, or 3 h, followed by cells being maintained in an incubator with 5 % CO_2 atmosphere at 37 °C for 15 min, 1 h, 3 h, or 24 h (RO) in 5 % FBS medium. Controls were maintained in an incubator with 5 % CO_2 atmosphere at 37 °C. After RO periods, images were captured using a digital camera connected to the microscope (Nikon Eclipse TE300, Nikon). Morphological changes during RO periods were analyzed and compared to OD groups.

Statistical Analysis

Data are expressed as mean ± SD. All results are representative of at least three independent experiments. One-way analysis of variance or Student's *t* test was applied to the means to determine statistical differences between experimental groups. Post hoc comparisons were performed by Tukey's test. Differences between mean values were considered significant at $p < 0.05$.

Results

OD Treatment Induces Apoptosis

For cells in 5 % FBS, viability was significantly reduced following a 3 h OD, while apoptosis increased during 1 and 3 h OD (Fig. 1a). Cells exposed to serum-free media, however, showed diminished viability with significant increase in apoptosis at the 1 and 3 h time points (Fig. 1b). These findings were supported by photomicrographs showing DAPI and PI staining results (Figs. S1 and S2).

C6 Glioma Cells Display Media-Specific Size Fluctuations

The majority of viable cells were sized in the M range, contrasting with the dead cells, which were frequently larger (Figs. 2 and **S3**). In 5 % FBS media, the viable cells decreased in size (from L to M) after 1 and 3 h OD (Figs. 2a and **S3**a). For dead cells, OD caused an increase in the number of S cells at the 1 h time point (Figs. 2a and **S3**a).

In serum-free media, although cell viability decreased with OD treatment, the remaining viable cells increased in size after 1 and 3 h OD (Figs. 2b and **S3**b). Meanwhile, following OD treatment, apoptotic cells displayed significant increases in cell size relative to the control apoptotic cells at the 1 and 3 h time points (Figs. 2b and **S3**b).

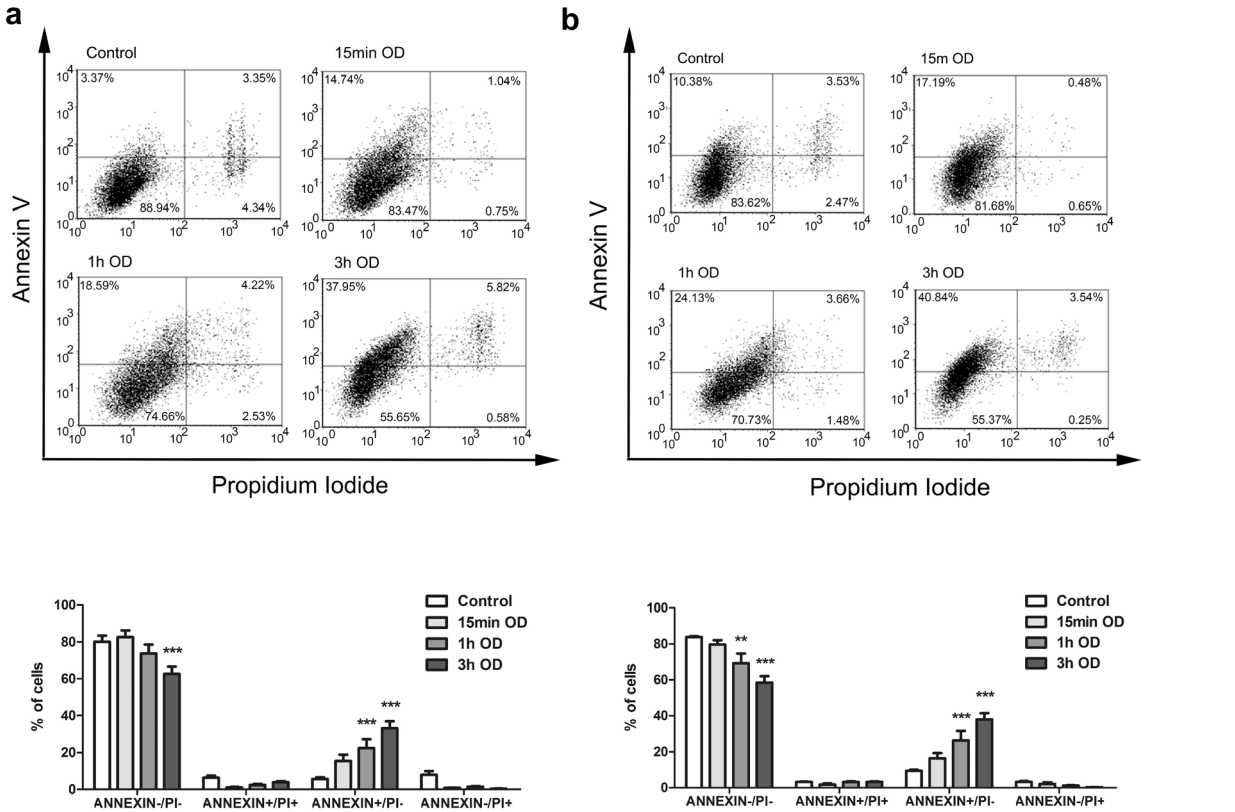

Fig. 1 OD treatment induces apoptotic cell death. *Dot-plot* analysis from flow cytometry of cells in **a** 5 % FBS medium or **b** serum-free medium. Percentage of cells according to viability and type of cell death: annexin V−/PI− (viable cells), annexin V+/PI+ (late apoptosis), annexin V+/PI− (apoptosis), and annexin V−/PI+ (necrosis). Data are represented as mean ± SEM ($n = 6$). $^{**}p < 0.01$, $^{***}p < 0.001$ vs. control

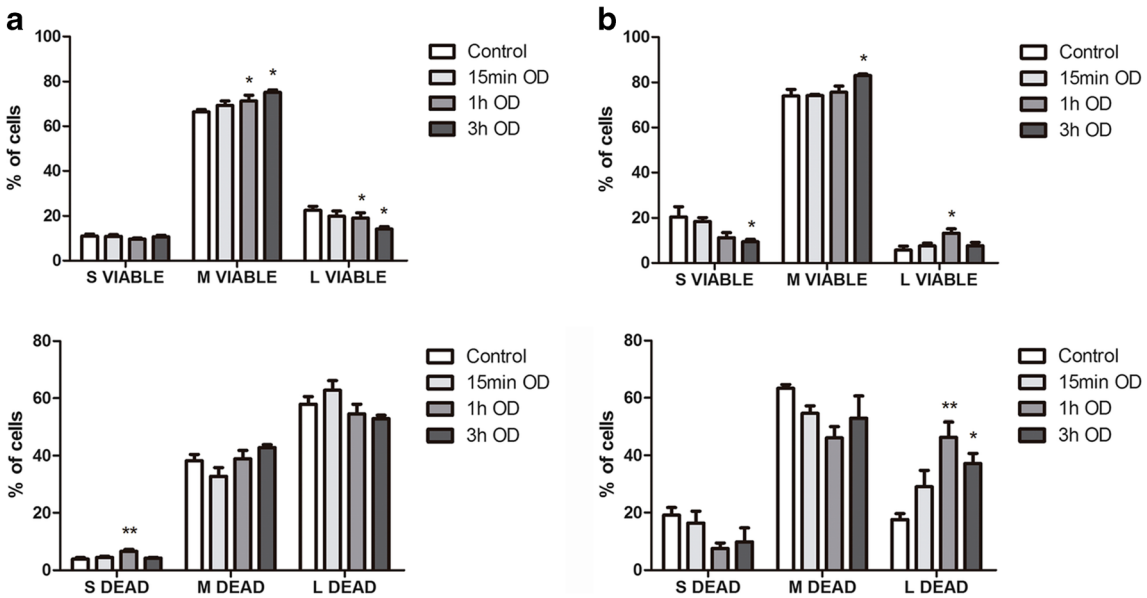

Fig. 2 Analysis of cell size. Cells were stained with annexin V and PI and categorized into three sizes: small [S], medium [M], and large [L]. Distribution of cell size in viable and dead cells in **a** 5 % FBS medium or **b** serum-free medium. Data are represented as mean ± SEM ($n = 6$). $^{*}p < 0.05$, $^{**}p < 0.01$ vs. control

Apoptotic Cell Granularity Increases in Serum-Free Media

The majority of viable cells in 5 % FBS media displayed regular granularity (G1) that remained unchanged after all OD time periods, while the majority of dead cells were observed in the G2 range (Figs. 3a and S4a).

In the control group of the serum-free media, the majority of viable cells displayed regular granularity (G1), with only a rare subpopulation of viable cells presenting as G2 (Figs. 3b and S4b). The number of viable cells presenting as G2 increased at the 15 min and 1 h OD time points, and this number appeared to decrease with OD duration (Figs. 3b and S4b). Regular granularity (G1) in the serum-free media group was also predominant in control dead cells; however, dead cells that had been exposed to OD exhibited increased granularity (Figs. 3b and S4b). These results suggested that cells exposed to serum-free media were more granular.

Mitochondrial Membrane Potential during OD

In the 5 % FBS group, a 3 h OD caused depolarization of the mitochondrial membrane in a subpopulation of cells, as reflected by the lower fluorescence intensity of MitoTracker Red on gate 2 (Fig. 4a). A small subpopulation of cells (gate 3) with hyperpolarized mitochondrial membrane increased after the 15 min OD (Fig. 4a).

In the serum-free group, depolarization occurred as early as 15 min OD and persisted during 1 and 3 h (Fig. 4b). The small subpopulation of cells with high hyperpolarized mitochondrial membrane (gate 3) increased during the 15 min and 1 h OD (Fig. 4b).

OD Alters Akt, VEGF, CD133, and Nestin Levels

Akt is involved in signaling pathways regulating differentiation/dedifferentiation and cell death control. During all OD times, p-Akt_{Ser473} levels were decreased, on both 5 % FBS and serum-free groups (Fig. 5). Akt levels remained the same as the control group.

To analyze morphological changes and stemness, cells were analyzed for VEGF levels using flow cytometry (Fig. 6a). Our results indicated an increase in VEGF levels in cells exposed to 1 h OD compared with the control group, also on both 5 % FBS and serum-free groups (Fig. 6a). VEGFR levels remained unchanged (data not shown).

CD133 and nestin are cell markers of cancer stem cells. For cells in serum-free medium, nestin and CD133 were significantly increased in 1 h OD (Fig. 6b, c). In 5 % FBS, there was a tendency of an increase in CD133 levels ($p = 0.0603$). GFAP was unaltered (Fig. 6d).

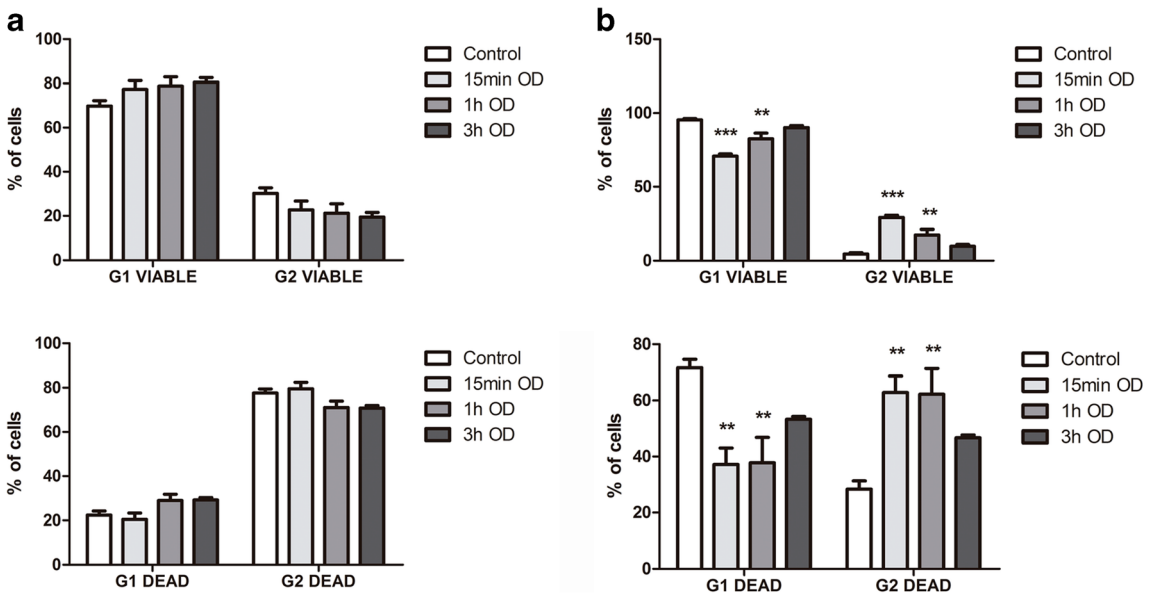

Fig. 3 Analysis of cell granularity. Cells were stained with annexin V and PI and categorized based on their granularity: regular [G1] and more granular [G2]. Distribution of granularity in viable and dead cells in **a** 5 % FBS medium or **b** serum-free medium. Data are represented as mean ± SEM ($n = 6$). $^{**}p < 0.01$, $^{***}p < 0.001$ vs. control

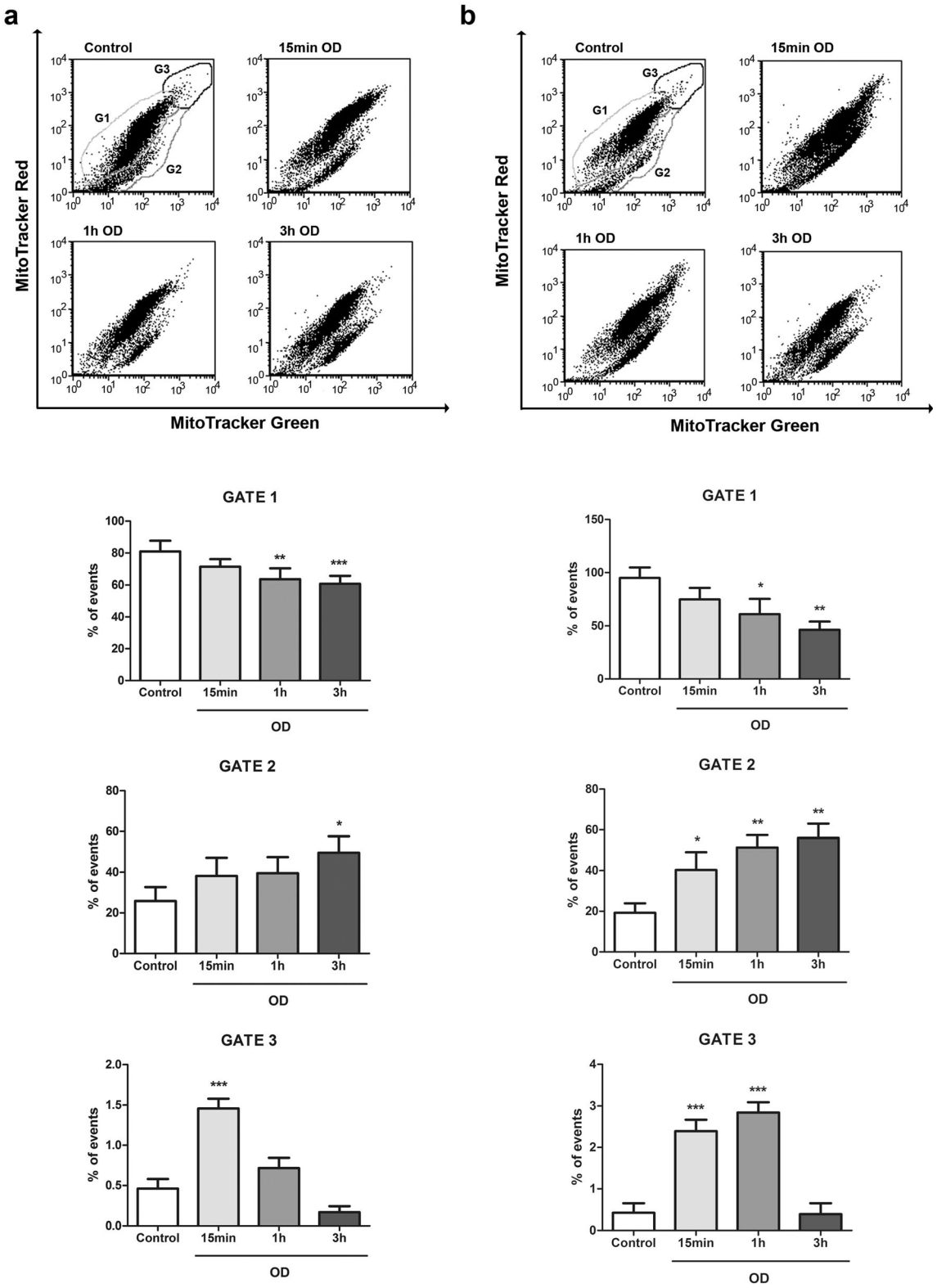

◀ **Fig. 4** *Dot-plot* analysis and distribution of gated events from flow cytometry of cells in **a** 5 % FBS medium or **b** serum-free medium stained with MitoTracker Green vs. MitoTracker Red. Cells were gated accordingly with different stained populations observed on control cells as shown on the *dot-plot* and as follows: *G1* gate 1; *G2* gate 2; *G3* gate 3. Data are represented as means ± SEM ($n = 6$). *$p < 0.05$, **$p < 0.01$, and ***$p < 0.001$ vs. control

Morphological and Protein Markers Changes Caused by Oxygen Deprivation and Reoxygenation

In C6 cells, 1 h OD in serum-free medium followed by 24 h RO increased CD133 and GFAP levels, while nestin remained unaltered (Fig. 7). Control cells displayed long spindles and evenly distributed processes (Figs. S1 and S2). After OD, cells became polygonal and processes decreased. As the time under OD conditions increased, the cells became oval-shaped and processes were absent (Figs. S1 and S2). As the duration of RO increased, cells became more long-spindled and displayed larger and thinner processes as well as decreased sizes (Figs. S3 and S4 and Table S1). These morphological changes were more pronounced during longer periods of hypoxia and RO.

Discussion

Tumor hypoxia is usually associated with poor patient prognosis and with resistance to therapy in GBMs [15]. In addition, this state contributes to glioblastoma cell proliferation, angiogenic drive, and metastasis/invasion [16, 17]. Hypoxic conditions also induce an immature phenotype on human neuroblastoma and breast cancer lines [18].

Hypoxia can lead to apoptotic or necrotic cell death with no consensus in the literature regarding the type of death [19–21]. Here, we exposed C6 cells to OD in the presence or absence of serum and observed that both groups presented mitochondrial membrane potential depolarization and cell death by apoptosis (Fig. 8).

Several studies demonstrated that hypoxia in vitro is a relatively strong inducer of apoptosis in colon carcinoma cell lines (HT29 and HCT116), oral cancer cells, glioma cell lines (U87, U251), and primary glioma cells [7, 12, 19]. One theory to explain the induction of apoptosis in cancer cells is that, due to tumor heterogeneity, some cells are more sensible to hypoxic DNA damage. Yao et al. [12] also hypothesized that mutational events are responsible for increased apoptosis susceptibility.

Previous studies have demonstrated that hypoxia activates Akt, which is in contrast with our findings. According to the literature, hypoxia induces phosphorylation of Akt at Ser473. In our study, however, $pAkt_{Ser473}$ levels were decreased during all OD times. Leszczynska et al. [22] demonstrated that activation of Akt occurred only in P53-null or mutant cells (HCT116 p53, H1299, OE21, and PSN1) but not in P53 wild-type (p53-wt) cells (RKO and HCT116). They suggest that p53 may be negatively regulating Akt activation on hypoxia and thus promoting apoptosis. C6 rat glioma cell line is p53-wt [23], and this could explain the decrease in Akt phosphorylation caused by hypoxia.

Zenali et al. [24] observed that increased granularity was related with an increase in CD133 expression. Cell size can be an important predictor of the metabolic state and metabolic reprogramming. CSCs are usually smaller than differentiated cancer cells, and the metabolic necessity is also lower [25]. Here, we show that hypoxia on the 5 % FBS group caused a decrease in viable cell size, but CSCs markers CD133 and nestin remained unaltered. This conditions were not sufficient to increase CD133 and nestin possibly because the environment was unsuitable, i.e., lacking autocrine factors that could induce cells to fully dedifferentiate.

On the other hand, hypoxia on the serum-free group caused an increase in viable cell size with increase in CD133 and nestin. Studies show a relationship between cell size and granularity on neural stem cells (NSCs): populations with increased size and granularity show enrichment of NSCs [26–28].

Increased mitochondrial membrane potential ($\Delta\psi m$) is proposed as a characteristic of CSCs [29]. Cells with intrinsically higher $\Delta\psi m$ demonstrate higher resistance to hypoxia and increased CD133 expression and show greater potential to form tumors [30]. Moreover, glioblastoma CSCs expressing CD133 exhibited elevated $\Delta\psi m$ [31]. These suggest that CSCs may have a different $\Delta\psi m$ when compared with differentiated carcinoma cells [29, 32]. Here, a subpopulation of C6 cells with high $\Delta\psi m$ was identified on normal culture conditions and on normoxia with serum-free medium. In the 5 % FBS group, 15 min OD increased this subpopulation of cells, and in the serum-free group, this increase was more pronounced and also appeared after 1 h OD. This result on the serum-free group corroborates with our hypothesis that the combination of hypoxia and the lack of serum promoted an increase in the CSCs population, since in the 1 h OD there was also an increase in CD133 and nestin expression.

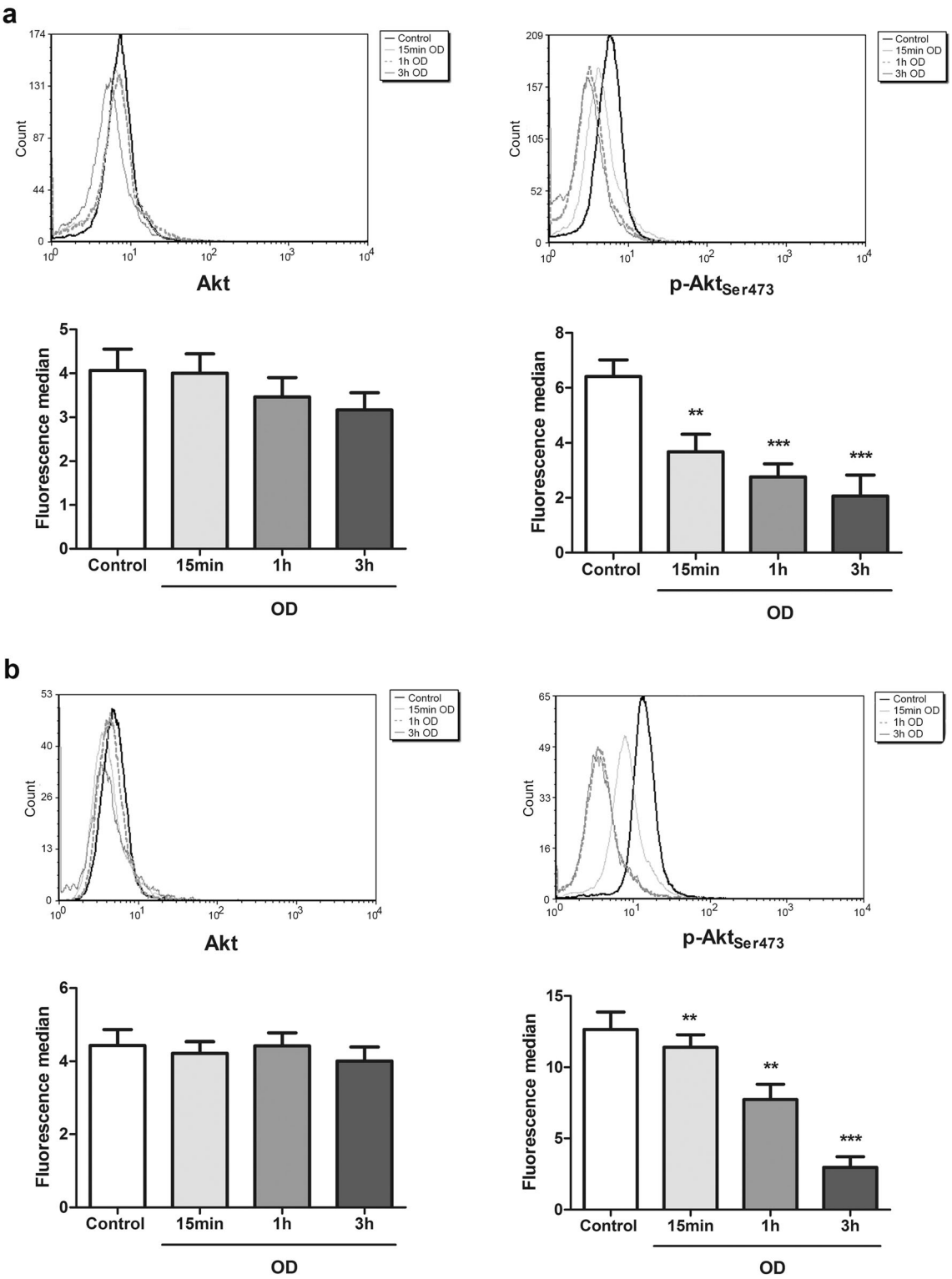

Fig. 5 Akt and p-Akt$_{Ser473}$ protein levels in C6 after OD, in **a** 5 % FBS and **b** serum-free media. Data are represented as means ± SEM (n = 6). $^{**}p < 0.01$ and $^{***}p < 0.001$ vs. control

VEGF helps maintain tumor cells in a stemness phenotype [33, 6]. After 1 h OD, VEGF levels increased in 5 % FBS and serum-free groups. These results confirm the morphological changes that occurred during OD:

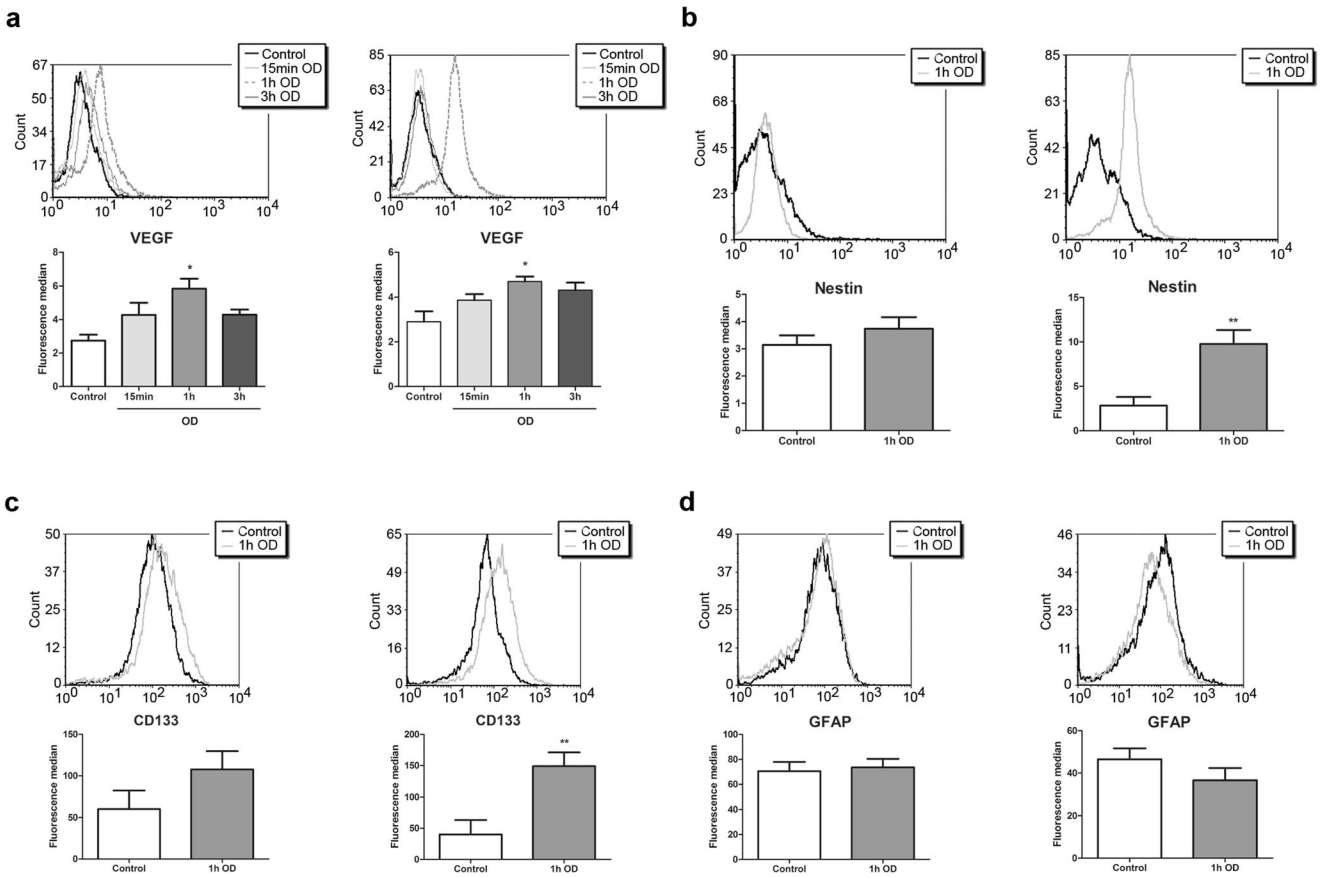

Fig. 6 Protein levels of **a** VEGF, **b** nestin, **c** CD133, and **d** GFAP in C6 cells after OD. On the *left side* of each protein level, the 5 % FBS group is represented, while the serum-free group is on the *right side*. Data are represented as mean ± SEM ($n = 6$). *$p < 0.05$ and **$p < 0.01$ vs. control

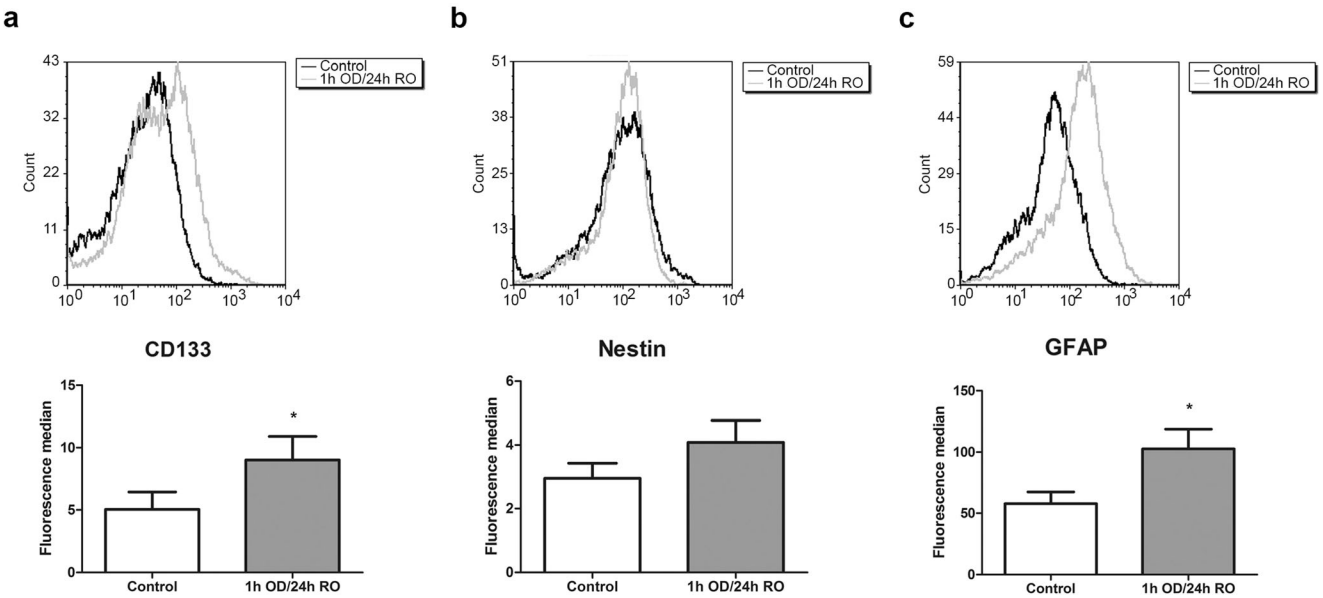

Fig. 7 Expression levels of **a** CD133, **b** nestin, and **c** GFAP after 1 h OD in serum free medium and 24 h RO in C6 cells. Data are represented as means ± SEM ($n = 6$). *$p < 0.05$ vs. control

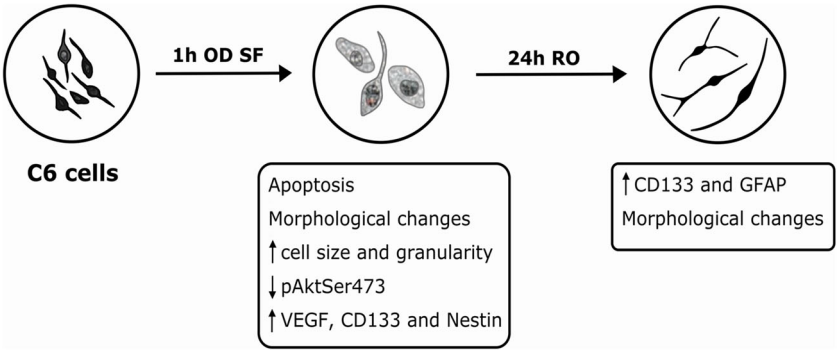

Fig. 8 Schematic illustration of the effects of in vitro oxygen deprivation in the absence of serum and of reoxygenation on C6 glioma cells

oval-shaped bodies and absence of cellular processes, a characteristic of stemness [7]. The serum-free group showed more profound changes in viable cell morphology than the 5 % FBS group. Moreover, nestin and CD133 levels increased after 1 h OD in the serum-free group, which is a characteristic of cancer stem cells. In the 5 % FBS group, however, nestin and CD133 levels remained unaltered after OD. Studies demonstrate that the absence of serum and the combination of basic fibroblast growth factor (bFGF) and platelet-derived growth factor (PDGF) seem to be able to maintain subpopulations of cancer stem cells [30, 34–37]. In addition, in vitro hypoxia can stimulate autocrine secretion of PDGF and bFGF [38]. The differences in our findings regarding the 5 % FBS and the serum-free groups highlight the importance of serum for cell dedifferentiation. In the presence of serum, hypoxia caused morphological changes characteristic of stem cells and increased VEGF levels, but did not induce dedifferentiation, since nestin and CD133 levels remained unaltered. The absence of serum in conjunction with hypoxia, however, seems to promote a favorable environment for cell dedifferentiation.

Segovia et al. [39] provide the evidence that C6 CSCs express proteins and mRNAs that are characteristic of both glia and neurons, and they can differentiate into both types of cells in vitro and in vivo. Li et al. [7] described that hypoxia induces dedifferentiation of differentiated glioma cells, causing them to acquire stemness. Moreover, neural precursors maintain undifferentiated phenotypes in low O_2 concentrations, while higher O_2 concentrations promote cellular differentiation.

Here, we showed that OD promoted C6 cell dedifferentiation, while reoxygenation appeared to cause differentiation of CSCs. The increase in GFAP levels and the cell morphology after 24 h RO supports this hypothesis. CD133 levels, however, also increased after 24 h RO, suggesting that some cells maintained stemness even in the presence of O_2, as occurs in the microenvironment of hypoxic tumors.

Therefore, models of GBM tumors in hypoxic conditions and the data presented in this study support the hypothesis that hypoxic niches contribute to GBM malignancy. Given that limited O_2 concentration is important for tumor progression and therapy resistance, studies of more efficient antitumoral strategies require increased understanding of the tumor microenvironment, which is characterized by lack of O_2.

Moreover, our study shows the importance of serum for in vitro analysis of the hypoxic tumoral microenvironment. Hypoxia in the absence of serum induced C6 cells to dedifferentiate to a CSCs phenotype, while the presence of serum caused subtle changes. Another important factor to be considered when studying in vitro hypoxia on cancer cells is p53 status. P53 mutations can confer apoptosis and chemotherapy resistance to cancer cells, and this can affect their response to hypoxia. We believe that the lack of consensus between different studies on hypoxia effects on tumor cells is due to varying approaches regarding these factors. Also, few studies analyze the reoxygenation period. In hypoxic tumors, reoxygenation can occur when cells receive oxygen from newly formed microvasculatures or when hypoxic-resistant cells migrate to more oxygenated areas. Therefore, analysis of reoxygenation in vitro is important to characterize those adaptive changes on cancer cells.

Regarding GBM, there needs to be greater understating of CSCs adaptations to the hypoxic microenvironment in order to develop effective treatments for this lethal tumor. Such knowledge can provide novel targets against therapy-resistant glioblastoma.

Compliance with Ethical Standards

Funding This study was funded by Conselho Nacional de Desenvolvimento Científico e Tecnológico (CNPq), Coordenação de Aperfeiçoamento de Pessoal de Nível Superior (Capes), and Fundação de Amparo à Pesquisa do Estado do Rio Grande do Sul (FAPERGS).

References

1. Oike T, Suzuki Y, K-i S, Shirai K, S-e N, Tamaki T, Nagaishi M, Yokoo H, Nakazato Y, Nakano T (2013) Radiotherapy plus concomitant adjuvant temozolomide for glioblastoma: Japanese mono-institutional results. PLoS One 8(11):e78943
2. Sengupta S, Marrinan J, Frishman C, Sampath P (2012) Impact of temozolomide on immune response during malignant glioma chemotherapy. Clin Dev Immunol 2012
3. Shen G, Shen F, Shi Z, Liu W, Hu W, Zheng X, Wen L, Yang X (2008) Identification of cancer stem-like cells in the C6 glioma cell line and the limitation of current identification methods. Vitro Cellular & Developmental Biology-Animal 44(7):280–289
4. Knizetova P, Ehrmann J, Hlobilkova A, Vancova I, Kalita O, Kolar Z, Bartek J (2008) Autocrine regulation of glioblastoma cell-cycle progression, viability and radioresistance through the VEGF-VEGFR2 (KDR) interplay. Cell Cycle 7(16):2553–2561
5. Bachelder RE, Wendt MA, Mercurio AM (2002) Vascular endothelial growth factor promotes breast carcinoma invasion in an autocrine manner by regulating the chemokine receptor CXCR4. Cancer Res 62(24):7203–7206
6. Hamerlik P, Lathia JD, Rasmussen R, Wu Q, Bartkova J, Lee M, Moudry P, Bartek J, Fischer W, Lukas J (2012) Autocrine VEGF–VEGFR2–Neuropilin-1 signaling promotes glioma stem-like cell viability and tumor growth. J Exp Med 209(3):507–520
7. Li P, Zhou C, Xu L, Xiao H (2013) Hypoxia enhances stemness of cancer stem cells in glioblastoma: an in vitro study. Int J Med Sci 10(4):399–407
8. Karamboulas C, Ailles L (2013) Developmental signaling pathways in cancer stem cells of solid tumors. Biochimica et Biophysica Acta (BBA)-General Subjects 1830(2):2481–2495
9. Swamydas M, Ricci K, Rego SL, Dréau D (2013) Mesenchymal stem cell-derived CCL-9 and CCL-5 promote mammary tumor cell invasion and the activation of matrix metalloproteinases. Cell Adhes Migr 7(3):315–324
10. Zhou X, Wang X, Qu F, Zhong Y, Lu X, Zhao P, Wang D, Huang Q, Zhang L, Li X (2009) Detection of cancer stem cells from the C6 glioma cell line. J Int Med Res 37(2):503–510
11. Ye X-Q, Wang G-H, Huang G-J, Bian X-W, Qian G-S, Yu S-C (2011) Heterogeneity of mitochondrial membrane potential: a novel tool to isolate and identify cancer stem cells from a tumor mass? Stem Cell Rev Rep 7(1):153–160
12. Yao K, Gietema J, Shida S, Selvakumaran M, Fonrose X, Haas N, Testa J, O'Dwyer P (2005) In vitro hypoxia-conditioned colon cancer cell lines derived from HCT116 and HT29 exhibit altered apoptosis susceptibility and a more angiogenic profile in vivo. Br J Cancer 93(12):1356–1363
13. Strasser U, Fischer G (1995) Quantitative measurement of neuronal degeneration in organotypic hippocampal cultures after combined oxygen/glucose deprivation. J Neurosci Methods 57(2):177–186
14. Cimarosti H, Rodnight R, Tavares A, Paiva R, Valentim L, Rocha E, Salbego C (2001) An investigation of the neuroprotective effect of lithium in organotypic slice cultures of rat hippocampus exposed to oxygen and glucose deprivation. Neurosci Lett 315(1):33–36
15. Keith B, Simon MC (2007) Hypoxia-inducible factors, stem cells, and cancer. Cell 129(3):465–472
16. Li Z, Bao S, Wu Q, Wang H, Eyler C, Sathornsumetee S, Shi Q, Cao Y, Lathia J, McLendon RE (2009) Hypoxia-inducible factors regulate tumorigenic capacity of glioma stem cells. Cancer Cell 15(6):501–513
17. Zagzag D, Lukyanov Y, Lan L, Ali MA, Esencay M, Mendez O, Yee H, Voura EB, Newcomb EW (2006) Hypoxia-inducible factor 1 and VEGF upregulate CXCR4 in glioblastoma: implications for angiogenesis and glioma cell invasion. Lab Investig 86(12):1221–1232
18. Axelson H, Fredlund E, Ovenberger M, Landberg G, Påhlman S (2005) Hypoxia-induced dedifferentiation of tumor cells—a mechanism behind heterogeneity and aggressiveness of solid tumors. In: Seminars in cell & developmental biology, vol 4. Elsevier, pp. 554–563
19. Nagaraj NS, Vigneswaran N, Zacharias W (2004) Hypoxia-mediated apoptosis in oral carcinoma cells occurs via two independent pathways. Mol Cancer 3(1):1
20. Harris AL (2002) Hypoxia—a key regulatory factor in tumour growth. Nat Rev Cancer 2(1):38–47
21. Weinmann M, Jendrossek V, Handrick R, Güner D, Goecke B, Belka C (2004) Molecular ordering of hypoxia-induced apoptosis: critical involvement of the mitochondrial death pathway in a FADD/caspase-8 independent manner. Oncogene 23(21): 3757–3769
22. Leszczynska KB, Foskolou IP, Abraham AG, Anbalagan S, Tellier C, Haider S, Span PN, O'Neill EE, Buffa FM, Hammond EM (2015) Hypoxia-induced p53 modulates both apoptosis and radiosensitivity via AKT. J Clin Invest 125(6):2385–2398
23. Asai A, Miyagi Y, Sugiyama A, Gamanuma M, Hong SI, Takamoto S, Nomura K, Matsutani M, Takakura K, Kuchino Y (1994) Negative effects of wild-type p53 and s-Myc on cellular growth and tumorigenicity of glioma cells. J Neuro-Oncol 19(3):259–268
24. Zenali MJ, Tan D, Li W, Dhingra S, Brown RE (2010) Stemness characteristics of fibrolamellar hepatocellular carcinoma: immunohistochemical analysis with comparisons to conventional hepatocellular carcinoma. Annals of Clinical & Laboratory Science 40(2):126–134
25. Li Q, Rycaj K, Chen X, Tang DG (2015) Cancer stem cells and cell size: a causal link? In: Seminars in cancer biology. Elsevier, pp. 191–199
26. Murayama A, Matsuzaki Y, Kawaguchi A, Shimazaki T, Okano H (2002) Flow cytometric analysis of neural stem cells in the developing and adult mouse brain. J Neurosci Res 69(6):837–847
27. Rietze RL, Valcanis H, Brooker GF, Thomas T, Voss AK, Bartlett PF (2001) Purification of a pluripotent neural stem cell from the adult mouse brain. Nature 412(6848):736–739
28. Narayanan G, Poonepalli A, Chen J, Sankaran S, Hariharan S, Yu YH, Robson P, Yang H, Ahmed S (2012) Single-cell mRNA profiling identifies progenitor subclasses in neurospheres. Stem Cells Dev 21(18):3351–3362
29. J-j D, Qiu W, Xu S-l, Wang B, X-z Y, Y-f P, Zhang X, X-w B, Yu S-c (2013) Strategies for isolating and enriching cancer stem cells: well begun is half done. Stem Cells Dev 22(16):2221–2239
30. Zheng X, Shen G, Yang X, Liu W (2007) Most C6 cells are cancer stem cells: evidence from clonal and population analyses. Cancer Res 67(8):3691–3697

31. Michelakis E, Sutendra G, Dromparis P, Webster L, Haromy A, Niven E, Maguire C, Gammer T-L, Mackey J, Fulton D (2010) Metabolic modulation of glioblastoma with dichloroacetate. Sci Transl Med 2(31):31ra34
32. Schieke SM, Ma M, Cao L, McCoy JP, Liu C, Hensel NF, Barrett AJ, Boehm M, Finkel T (2008) Mitochondrial metabolism modulates differentiation and teratoma formation capacity in mouse embryonic stem cells. J Biol Chem 283(42):28506–28512
33. Seton-Rogers S (2011) Cancer stem cells: VEGF promotes stemness. Nat Rev Cancer 11(12):831–831
34. Yuan X, Curtin J, Xiong Y, Liu G, Waschsmann-Hogiu S, Farkas DL, Black KL, John SY (2004) Isolation of cancer stem cells from adult glioblastoma multiforme. Oncogene 23(58):9392–9400
35. Galli R, Binda E, Orfanelli U, Cipelletti B, Gritti A, De Vitis S, Fiocco R, Foroni C, Dimeco F, Vescovi A (2004) Isolation and characterization of tumorigenic, stem-like neural precursors from human glioblastoma. Cancer Res 64(19):7011–7021
36. Sakaki T, Yamada K, Otsuki H, Yuguchi T, Kohmura E, Hayakawa T (1995) Brief exposure to hypoxia induces bFGF mRNA and protein and protects rat cortical neurons from prolonged hypoxic stress. Neurosci Res 23(3):289–296
37. Kyurkchiev D (2014) Cancer stem cells from glioblastoma multiforme: culturing and phenotype. Stem Cells 2(1):3
38. Freyhaus H, Dagnell M, Leuchs M, Vantler M, Berghausen EM, Caglayan E, Weissmann N, Dahal BK, Schermuly RT, Östman A (2011) Hypoxia enhances platelet-derived growth factor signaling in the pulmonary vasculature by down-regulation of protein tyrosine phosphatases. Am J Respir Crit Care Med 183(8):1092–1102
39. Segovia J, Lawless GM, Tillakaratne NJ, Brenner M, Tobin AJ (1994) Cyclic AMP decreases the expression of a neuronal marker (GAD67) and increases the expression of an astroglial marker (GFAP) in C6 cells. J Neurochem 63(4): 1218–1225